THE ROLE OF EULER PARAMETERS IN ROBOT CONTROL

Fabrizio Caccavale, Bruno Siciliano, and Luigi Villani

ABSTRACT

Euler parameters constitute a well-known nonminimal singularity-free representation of rigid body orientation. This paper is aimed at illustrating the role of Euler parameters in robot control; namely, the kinematic control, dynamic control and impedance control problems are surveyed in a unifying perspective, where robot's end-effector orientation displacements are described in terms of Euler parameters. The advantages over the Euler angles typically used in the operational space framework are demonstrated.

KeyWords: Euler parameters, robots, kinematic control, dynamic control, impedance control.

I. INTRODUCTION

Robots are typically used to manipulate objects in space, and thus a robotic task requires the specification of the mutual position and orientation between the robot's end effector and an object. Once a base frame is established, a suitable frame attached to the end effector is considered whose position is uniquely described by the Cartesian coordinates of the origin, while its orientation can be represented in various ways.

A complete representation of orientation is given by the rotation matrix. Its columns are the unit vectors of the end-effector frame expressed in the base frame, yielding 9 parameters subject to 6 orthonormality constraints. On the other hand, minimal representations of orientation are defined by 3 parameters, i.e. Euler angles. These are rather common in robot control, since they are at the basis of the so-called operational space concept [1]; a robotic task is described in this space in terms of at most $m \leq 6$ degrees of freedom vs. the $n \geq m$ degrees of mobility characterizing the joint space [2].

Classical control problems tackled in the operational space include:

- *kinematic control*, i.e. compute the joint trajectories corresponding to an end-effector trajectory given in the operational space, which then constitute the reference inputs to some joint feedback control scheme [3];
- *dynamic control*, i.e. compute the joint control torques guaranteeing tracking of a given end-effector trajectory, by feeding back directly end-effector motion variables [4];
- *impedance control*, i.e. compute the joint control torques guaranteeing a given mechanical impedance behaviour when the end effector interacts with the environment, by feeding back end-effector motion and force variables [5].

In spite of their popularity, not only do Euler angles suffer from the drawback of representation singularities affecting the motion control problem, but also consistency with task geometry is not ensured when the interaction control problem is of concern.

An alternative nonminimal representation of orientation can be considered in terms of 4 parameters with 1 norm constraint which is based on a geometric description of the rotation in terms of an equivalent angle and axis. Such are the *Euler parameters*, viz. the unit quaternion, which provide a global singularity-free parameterization of the special orthogonal group of rotations [6].

Inspired by the work in [7], recently, Euler parameters have been adopted as a valid alternative to Euler angles to solve the kinematic control [8], dynamic contro [9] and impedance control [10] problems. The respective developments are here surveyed in a unifying perspective with the goal of demonstrating the advantages and simplicity of expressing orientation displacements in terms of Euler parameters.

II. EULER PARAMETERS

The location of a rigid body in space is typically described in terms of the (3×1) position vector $\boldsymbol{p}$ and the (3×3) rotation matrix $\boldsymbol{R}$ describing the origin and the orientation of a frame attached to the body with respect to a fixed base frame.

The body linear velocity is described by the time derivative of the position vector, i.e. $\dot{\boldsymbol{p}}$, while its angular velocity $\boldsymbol{\omega}$ can be defined through the time derivative of the

Manuscript received March 2, 1999; accepted April 14, 1999.

The authors are with the Dipartimento Informatica Sistemistica, Università degli Studi di Nnapoli, Federico II, 80125 Napoli, Italy.

rotation matrix by the relationship

$$\dot{\boldsymbol{R}} = \boldsymbol{S}(\boldsymbol{\omega})\boldsymbol{R}\,, \tag{1}$$

where $\boldsymbol{S}(\cdot)$ is the skew-symmetric matrix operator performing the cross product between two (3×1) vectors.

A minimal representation of orientation can be obtained by using a set of three Euler angles $\boldsymbol{\varphi} = [\alpha \;\; \beta \;\; \gamma]^T$. Among the 12 possible definitions of Euler angles, without loss of generality, the *XYZ* representation is considered leading to the rotation matrix

$$\boldsymbol{R}(\boldsymbol{\varphi}) = \boldsymbol{R}_x(\alpha)\boldsymbol{R}_y(\boldsymbol{\beta})\boldsymbol{R}_z(\gamma) \tag{2}$$

where $\boldsymbol{R}_x$, $\boldsymbol{R}_y$, $\boldsymbol{R}_z$ are the matrices of the elementary rotations about three independent axes of successive frames.

The relationship between the time derivative of the Euler angles $\dot{\boldsymbol{\varphi}}$ and the body angular velocity $\boldsymbol{\omega}$ is given by

$$\boldsymbol{\omega} = \boldsymbol{T}(\boldsymbol{\varphi})\dot{\boldsymbol{\varphi}}\,, \tag{3}$$

where the transformation matrix $\boldsymbol{T}$ becomes singular at the so-called *representation singularities*. In these configurations, it is not possible to describe an arbitrary angular velocity with a set of Euler angles time derivatives. Notice that all Euler angles representations suffer from two representation singularities occurring when the first and last axes of rotation in the sequence, e.g. as in (2), lie along the same direction; also, at a representation singularity, the extraction of the Euler angles corresponding to a given rotation matrix is not unique.

To solve the representation singularity problem, an alternative representation of orientation can be obtained in terms of a rotation angle ϑ about an axis in space described by the (3×1) unit vector $\boldsymbol{r}$. The resulting rotation matrix is

$$\boldsymbol{R}(\vartheta, \boldsymbol{r}) = \cos\vartheta\boldsymbol{I} + (1 - \cos\vartheta)\boldsymbol{r}\boldsymbol{r}^T - \sin\vartheta\boldsymbol{S}(\boldsymbol{r}) \tag{4}$$

where $\boldsymbol{I}$ is the (3×3) identity matrix.

It is clear that $\boldsymbol{R}(-\vartheta, -\boldsymbol{r}) = \boldsymbol{R}(\vartheta, \boldsymbol{r})$, i.e. a rotation by $-\vartheta$ about $-\boldsymbol{r}$ cannot be distinguished from a rotation by ϑ about $\boldsymbol{r}$; hence, the angle/axis representation is not unique. Also, if $\vartheta = 0$ then $\boldsymbol{r}$ is arbitrary; this is a singularity of the angle/axis representation. These drawbacks can be overcome by a four-parameter representation; namely, the *Euler parameters* or unit quaternion defined as [11]

$$\eta = \cos\frac{\vartheta}{2}$$

$$\varepsilon = \sin\frac{\vartheta}{2}\boldsymbol{r}\,. \tag{5}$$

Notice that the scalar part and the vector part of the Euler parameters are constrained by

$$\eta^2 + \varepsilon^T\varepsilon = 1, \tag{6}$$

and $\eta \geq 0$ for $\vartheta \in [-\pi, \pi]$. It is worth remarking that, differently from the angle/axis representation, a rotation by $-\vartheta$ about $-\boldsymbol{r}$ gives the same Euler parameters as those associated with a rotation by ϑ about $\boldsymbol{r}$; this solves the above nonuniqueness problem. Also, no singularity occurs.

The rotation matrix corresponding to a given set of Euler parameters is

$$\boldsymbol{R}(\eta, \varepsilon) = (\eta^2 - \varepsilon^T\varepsilon)\boldsymbol{I} + 2\varepsilon\varepsilon^T - 2\eta\boldsymbol{S}(\varepsilon). \tag{7}$$

Several algorithms exist to extract the Euler parameters from a given rotation matrix; an efficient one is reported in [12].

The relationship between the time derivative of the Euler parameters and the body angular velocity $\boldsymbol{\omega}$ is established by the so-called propagation rule:

$$\dot{\eta} = -\frac{1}{2}\varepsilon^T\boldsymbol{\omega} \tag{8}$$

$$\dot{\varepsilon} = \frac{1}{2}\boldsymbol{E}(\eta, \varepsilon)\boldsymbol{\omega} \tag{9}$$

with

$$\boldsymbol{E}(\eta, \varepsilon) = \eta\boldsymbol{I} - \boldsymbol{S}(\varepsilon)\,. \tag{10}$$

Consider now two frames, conventionally labeled 1 and 2. Let $\boldsymbol{R}_1$ and $\boldsymbol{R}_2$ respectively denote the rotation matrices expressing the orientation of the two frames with respect to the base frame. Then, the mutual orientation between the two frames can be described by the rotation matrix

$$\boldsymbol{R}_2^1 = \boldsymbol{R}_1^T\boldsymbol{R}_2\,. \tag{11}$$

As usual, a superscript denotes the frame to which a quantity (vector or matrix) is referred; the superscript is dropped whenever a quantity is referred to the base frame.

The Euler parameters describing the mutual orientation can be either extracted directly from $\boldsymbol{R}_2^1$ or computed by composition of the Euler parameters $\{\eta_1, -\varepsilon_1\}$ and $\{\eta_2, \varepsilon_2\}$ that can be extracted from $\boldsymbol{R}_1^T$ and $\boldsymbol{R}_2$, respectively, i.e.

$$\eta_{21} = \eta_1\eta_2 + \varepsilon_1^T\varepsilon_2 \tag{12}$$

$$\varepsilon_{21}^1 = \eta_1\varepsilon_2 - \eta_2\varepsilon_1 - \boldsymbol{S}(\varepsilon_1)\varepsilon_2 \tag{13}$$

where the double subscript denotes that a mutual orientation is of concern; the vector part of the Euler parameters has been referred to frame 1, but it is easy to prove that $\varepsilon_{21}^1 = \varepsilon_{21}^2$. Notice that $\boldsymbol{R}_2^1$ is related to $\{\eta_{21}, \varepsilon_{21}^1\}$ through a relationship formally equal to (7).

The differential kinematics relationship corre-

sponding to (1) is

$$\dot{\boldsymbol{R}}_2^1 = \boldsymbol{S}(\Delta\boldsymbol{\omega}_{21}^1)\boldsymbol{R}_2^1 , \tag{14}$$

where

$$\Delta\boldsymbol{\omega}_{21}^1 = \boldsymbol{\omega}_2^1 - \boldsymbol{\omega}_1^1 = \boldsymbol{R}_1^T(\boldsymbol{\omega}_2 - \boldsymbol{\omega}_1) \tag{15}$$

is the angular velocity of frame 2 relative to frame 1, which has been referred to frame 1; the operator Δ has been introduced to denote that a vector difference has been taken. Accordingly, the differential kinematics relationship corresponding to (8), (9) becomes

$$\dot{\eta}_{21} = -\frac{1}{2}\boldsymbol{\varepsilon}_{21}^{1T}\Delta\boldsymbol{\omega}_{21}^1 \tag{16}$$

$$\dot{\boldsymbol{\varepsilon}}_{21}^1 = \frac{1}{2}\boldsymbol{E}(\eta_{21}, \boldsymbol{\varepsilon}_{21}^1)\Delta\boldsymbol{\omega}_{21}^1 \tag{17}$$

with $\boldsymbol{E}$ defined as in (10).

III. KINEMATIC CONTROL

Robot *kinematic control* consists of solving the motion control problem into two stages, i.e., the desired end-effector trajectory is transformed via the inverse kinematics into corresponding joint trajectories, which then constitute the reference inputs to some joint space control scheme [3]. This approach differs from operational space control [1] in the sense that manipulator kinematics is handled outside the control loop thus allowing the problem of kinematic singularities and/or redundancy to be solved separately from the motion control problem. Moreover, most built-in controllers of industrial robots are based on joint servos and thus they can be easily embedded into a kinematic control strategy.

The key point of kinematic control is the solution to the inverse kinematics problem. If the manipulator has simple geometry and is nonredundant with respect to the given task, closed-form solutions can be found for the joint variables but special care has to be paid for the occurrence of singular configurations. On the other hand, for general manipulator structures, the inverse kinematics problem can be tackled by resorting to differential kinematics and thus inverting the end-effector motion into an equivalent joint motion. This is based on the manipulator Jacobian, which is the fundamental tool for analyzing kinematic singularities and/or redundancy.

The direct kinematics equation for a serial-chain robot manipulator can be written in terms of the vector

$$\boldsymbol{p}_e = \boldsymbol{p}_e(\boldsymbol{q}) \tag{18}$$

and the rotation matrix

$$\boldsymbol{R}_e = \boldsymbol{R}_e(\boldsymbol{q}) \tag{19}$$

where $\boldsymbol{q}$ is the $(n \times 1)$ vector of joint variables, and $\boldsymbol{p}_e$ and $\boldsymbol{R}_e$ respectively denote the position and the orientation of the end-effector frame.

The differential kinematics is characterized by the relationship between the end-effector linear velocity $\dot{\boldsymbol{p}}_e$ and angular velocity $\boldsymbol{\omega}_e$ and the joint velocities $\dot{\boldsymbol{q}}$, i.e.

$$\begin{bmatrix} \dot{\boldsymbol{p}}_e \\ \boldsymbol{\omega}_e \end{bmatrix} = \boldsymbol{J}(\boldsymbol{q})\dot{\boldsymbol{q}} \tag{20}$$

where $\boldsymbol{J}$ is the manipulator geometric Jacobian [2]. In the general case ($m = 6$), this is a $(6 \times n)$ matrix which may be singular. When $n > 6$, kinematic redundancy exists which can be handled by suitable inverse kinematics techniques, e.g. [13]. On the other hand, when rank($\boldsymbol{J}$) < 6, a kinematic singularity occurs and robustness of inverse kinematics solutions can be gained as in, e.g. [14]. Since the focus of the present work is on the problems related to orientation representation, without loss of generality, the Jacobian is assumed to be a nonsingular square matrix.

Let $\boldsymbol{p}_d$ and $\boldsymbol{R}_d$ denote the desired end-effector trajectory. The inverse kinematics problem consists of computing the corresponding joint trajectories $\boldsymbol{q}$ which are solution of the kinematics equation. Analytical inverse kinematics solutions can be found only for nonredundant manipulators having a simple geometry, e.g. with a spherical wrist.

An effective solution which is applicable to any kinematic structure is based on the time integration of the joint velocities obtained by inversion of (20). In order to overcome the typical numerical drift concerned with discrete-time implementation of this solution, a closed-loop inverse kinematics (CLIK) algorithm can be devised which acts upon an error characterizing the displacement between the desired and the end-effector trajectory computed via (18), (19).

Let

$$\Delta\boldsymbol{p}_{de} = \boldsymbol{p}_d - \boldsymbol{p}_e(\boldsymbol{q}) \tag{21}$$

denote the end-effector position error. The end-effector orientation error depends on the choice of the orientation description. In the case of Euler angles, the error is simply

$$\Delta\boldsymbol{\varphi}_{de} = \boldsymbol{\varphi}_d - \boldsymbol{\varphi}_e(\boldsymbol{q}) \tag{22}$$

where $\boldsymbol{\varphi}_d$ and $\boldsymbol{\varphi}_e$ denote the desired and current quantities, respectively. Notice that the computation of $\boldsymbol{\varphi}_e(\boldsymbol{q})$ requires the extraction of the Euler angles from the end-effector rotation matrix $\boldsymbol{R}_e$ via inversion formulae, which suffer from representation singularities though.

The joint velocity algorithmic solution is given by

$$\dot{\boldsymbol{q}} = \boldsymbol{J}_A^{-1}(\boldsymbol{q})\begin{bmatrix} \dot{\boldsymbol{p}}_d + k_{P_p}\Delta\boldsymbol{p}_{de} \\ \dot{\boldsymbol{\varphi}}_d + k_{P_o}\Delta\boldsymbol{\varphi}_{de} \end{bmatrix} \tag{23}$$

where k_{Pp} and k_{Po} are suitable positive gains, and $\boldsymbol{J}_A$ is the analytical Jacobian [2] that is related to the geometric Jacobian by the relationship

$$\boldsymbol{J}_A = \begin{bmatrix} \boldsymbol{I} & \boldsymbol{O} \\ \boldsymbol{O} & \boldsymbol{T}^{-1}(\boldsymbol{\varphi}) \end{bmatrix} \boldsymbol{J} \tag{24}$$

with $\boldsymbol{T}$ as in (3) and $\boldsymbol{O}$ is the (3×3) null matrix. Note that $\boldsymbol{J}_A$ is singular at a representation singularity, where it is not possible to describe an arbitrary set of Euler angles time derivatives with a set of joint velocities.

In view of (21), (22), substituting (23) into (20) gives

$$\Delta\dot{\boldsymbol{p}}_{de} + k_{P_p}\Delta\boldsymbol{p}_{de} = \boldsymbol{0} \tag{25}$$

$$\Delta\dot{\boldsymbol{\varphi}}_{de} + k_{P_o}\Delta\boldsymbol{\varphi}_{de} = \boldsymbol{0}\,. \tag{26}$$

It is easy to see that system (25) is exponentially stable, implying that $\Delta\boldsymbol{p}_{de}$ converges to zero. Likewise, system (26) is exponentially stable as long as no representation singularity occurs.

In order to devise an inverse kinematics scheme based on Euler parameters, a suitable end-effector orientation error shall be defined. Let $\{\eta_d, \boldsymbol{\varepsilon}_d\}$ and $\{\eta_e(\boldsymbol{q}), \boldsymbol{\varepsilon}_e(\boldsymbol{q})\}$ represent the Euler parameters associated with $\boldsymbol{R}_d$ and $\boldsymbol{R}_e(\boldsymbol{q})$, respectively. The mutual orientation can be expressed in terms of the Euler parameters $\{\eta_{de}, \boldsymbol{\varepsilon}^e_{de}\}$ via the formulae (12), (13). The end-effector orientation error can be defined as

$$\boldsymbol{\varepsilon}_{de} = R_e\boldsymbol{\varepsilon}^e_{de} \tag{27}$$

which has been conveniently referred to the base frame.

The joint velocity algorithmic solution is given by

$$\dot{\boldsymbol{q}} = \boldsymbol{J}^{-1}(\boldsymbol{q}) \begin{bmatrix} \dot{\boldsymbol{p}}_d + k_{P_p}\Delta\boldsymbol{p}_{de} \\ \boldsymbol{\omega}_d + k_{P_o}\boldsymbol{\varepsilon}_{de} \end{bmatrix}. \tag{28}$$

It is worth pointing out that in (28), differently from the previous Euler angles-based algorithm in (23), the geometric Jacobian appears in lieu of the analytical Jacobian, and thus representation singularities cannot occur.

In view of (21), (27), substituting (28) into (20) gives (25) and

$$\Delta\boldsymbol{\omega}_{de} + k_{P_o}\boldsymbol{\varepsilon}_{de} = \boldsymbol{0} \tag{29}$$

with $\Delta\boldsymbol{\omega}_{de}$ as in (15). It should be observed that now the orientation error equation is not homogeneous in $\boldsymbol{\varepsilon}_{de}$ since it contains the end-effector angular velocity error instead of the time derivative of the orientation error.

To study stability of system (29), consider the positive definite Lyapunov function candidate

$$V_1 = (\eta_{de} - 1)^2 + \boldsymbol{\varepsilon}^T_{de}\boldsymbol{\varepsilon}_{de}\,. \tag{30}$$

Using (27), in view of the propagation rule (16), (17), the time derivative of V_1 along the trajectories of system (29) is given by

$$\dot{V}_1 = -\,k_{P_o}\boldsymbol{\varepsilon}^T_{de}\boldsymbol{\varepsilon}_{de} \tag{31}$$

which is negative definite, implying that $\boldsymbol{\varepsilon}_{de}$ converges to zero.

The block scheme of the resulting CLIK algorithm using the Euler parameters is shown in Fig. 1.

IV. DYNAMIC CONTROL

Even though kinematic control is a congenial strategy used by industrial robots performing simple tasks, e.g. pick-and-place, operational space control becomes essential to execute complex tasks, e.g. those requiring interaction between the end effector and the environment. In such a case, a feedback loop is closed directly on operational space variables, and thus no preliminary inverse kinematics is required.

In order to cope with the nonlinear and coupled nature of the manipulator dynamic model, *dynamic control* can be pursued which consists of designing a model-based compensating action which globally linearizes and decouples the mechanical system in terms of a resolved operational space acceleration [4]; this is chosen on the basis of the end-effector position/orientation and velocity feedback so as to ensure stable tracking of the desired trajectory.

The dynamic model of a robot manipulator can be written in the joint space as

$$\boldsymbol{B}(\boldsymbol{q})\ddot{\boldsymbol{q}} + \boldsymbol{C}(\boldsymbol{q}, \dot{\boldsymbol{q}})\dot{\boldsymbol{q}} + \boldsymbol{d}(\boldsymbol{q}, \dot{\boldsymbol{q}}) + \boldsymbol{g}(\boldsymbol{q}) = \boldsymbol{\tau} - \boldsymbol{J}^T(\boldsymbol{q})\boldsymbol{h}\,, \tag{32}$$

where $\boldsymbol{B}$ is the $(n \times n)$ symmetric positive definite inertia matrix, $\boldsymbol{C}\dot{\boldsymbol{q}}$ is the $(n \times 1)$ vector of Coriolis and centrifugal torques, $\boldsymbol{d}$ is the $(n \times 1)$ vector of friction torques, $\boldsymbol{g}$ is the $(n \times 1)$ vector of gravitational torques, τ is the $(n \times 1)$ vector of driving torques, and $\boldsymbol{h} = [\boldsymbol{f}^T\ \boldsymbol{\mu}^T]^T$ is the (6×1) vector of contact forces and moments exerted by the end effector on the environment. For the purpose of this section, it is

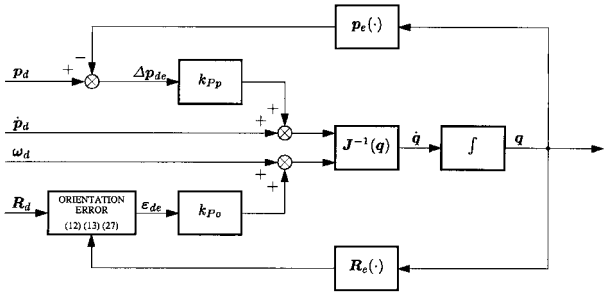

Fig. 1. Block scheme of CLIK algorithm.

assumed that $\boldsymbol{h} = \boldsymbol{0}$, i.e. no contact with the environment occurs.

According to the well-known concept of inverse dynamics, the driving torques can be chosen as

$$\boldsymbol{\tau} = \boldsymbol{B}(\boldsymbol{q})\boldsymbol{J}^{-1}(\boldsymbol{q})(\boldsymbol{a} - \dot{\boldsymbol{J}}(\boldsymbol{q}, \dot{\boldsymbol{q}})\dot{\boldsymbol{q}}) + \boldsymbol{C}(\boldsymbol{q}, \dot{\boldsymbol{q}})\dot{\boldsymbol{q}} + \boldsymbol{d}(\boldsymbol{q}, \dot{\boldsymbol{q}}) + \boldsymbol{g}(\boldsymbol{q}) , \tag{33}$$

where $\boldsymbol{a}$ is a new control input, and perfect dynamic compensation has been assumed; to this purpose, note that it is reasonable to assume accurate compensation of the dynamic terms in the model (32), e.g. as obtained by a parameter identification technique [15].

In deriving (33), a nonredundant manipulator ($n = 6$) moving in a singularity-free region of the workspace has been considered to compute the inverse of the Jacobian. A damped least-squares inverse can be adopted to gain robustness in the neighbourhood of kinematic singularities [16], whereas a pseudoinverse can be used in the redundant case ($n > 6$) in conjunction with a suitable term in the null space of the Jacobian describing the internal motion of the manipulator [17].

The vector $\boldsymbol{a}$ represents a resolved acceleration [4] which can be partitioned into its linear and angular components, i.e. $\boldsymbol{a} = [\boldsymbol{a}_p^T \;\; \boldsymbol{a}_o^T]^T$. Substituting the control law (33) in (32) and accounting for the time derivative of (20) gives

$$\ddot{\boldsymbol{p}}_e = \boldsymbol{a}_p \tag{34}$$

$$\dot{\boldsymbol{\omega}}_e = \boldsymbol{a}_o \, . \tag{35}$$

The goal is to design $\boldsymbol{a}_p$ and $\boldsymbol{a}_o$ so as to ensure tracking of the desired end-effector trajectory.

The resolved linear acceleration can be chosen as

$$\boldsymbol{a}_p = \ddot{\boldsymbol{p}}_d + k_{Vp}\Delta\dot{\boldsymbol{p}}_{de} + k_{Pp}\Delta\boldsymbol{p}_{de} \tag{36}$$

where $\Delta\boldsymbol{p}_{de}$ is defined in (21), and k_{Vp}, k_{Pp} are suitable positive feedback gains. Substituting (36) into (34) gives the closed-loop dynamic behaviour of the position error

$$\Delta\ddot{\boldsymbol{p}}_{de} + k_{Vp}\Delta\dot{\boldsymbol{p}}_{de} + k_{Pp}\Delta\boldsymbol{p}_{de} = \boldsymbol{0} \, . \tag{37}$$

The system (37) is exponentially stable, and thus tracking of $\boldsymbol{p}_d$ and $\dot{\boldsymbol{p}}_d$ is ensured.

As regards the resolved angular acceleration, $\boldsymbol{a}_o$ can be chosen in different ways, depending on the definition of end-effector orientation error used. According to the classical operational space approach [1], and accounting for the time derivative of (3), the resolved angular acceleration can be chosen as

$$\boldsymbol{a}_o = \boldsymbol{T}(\boldsymbol{\varphi}_e)(\ddot{\boldsymbol{\varphi}}_d + k_{V_o}\Delta\dot{\boldsymbol{\varphi}}_{de} + k_{P_o}\Delta\boldsymbol{\varphi}_{de}) + \dot{\boldsymbol{T}}(\boldsymbol{\varphi}_e, \dot{\boldsymbol{\varphi}}_e)\dot{\boldsymbol{\varphi}}_e \tag{38}$$

where $\Delta\boldsymbol{\varphi}_{de}$ is defined in (22), and k_{Vo}, k_{Po} are suitable positive feedback gains. Substituting (38) into (35) gives the closed-loop dynamic behaviour of the orientation error

$$\Delta\ddot{\boldsymbol{\varphi}}_{de} + k_{Vo}\Delta\dot{\boldsymbol{\varphi}}_{de} + k_{Po}\Delta\boldsymbol{\varphi}_{de} = \boldsymbol{0} \tag{39}$$

where the matrix $\boldsymbol{T}(\boldsymbol{\varphi}_e)$ shall be nonsingular. The system (39) is exponentially stable, i.e. tracking of $\boldsymbol{\varphi}_d$ and $\dot{\boldsymbol{\varphi}}_d$ is ensured, which in turn implies tracking of $\boldsymbol{R}_d$ and $\boldsymbol{\omega}_d$.

The above Euler angles-based control scheme becomes ill-conditioned when the actual end-effector orientation $\boldsymbol{\varphi}_e$ becomes close to a representation singularity. In order to mitigate this drawback, an alternative orientation error can be adopted which is based on the Euler angles extracted from the rotation matrix describing the mutual orientation between the desired and the actual end-effector frame; the advantage is that representation singularities occur only for large orientation errors as long as a proper set of Euler angles is chosen [9].

In order to overcome the problem of representation singularities, the orientation error can be defined in terms of the Euler parameters as in (27). Accordingly, the resolved angular acceleration can be chosen as

$$\boldsymbol{a}_o = \dot{\boldsymbol{\omega}}_d + k_{Vo}\Delta\boldsymbol{\omega}_{de} + k_{Po}\boldsymbol{\varepsilon}_{de} \tag{40}$$

where k_{Vo}, k_{Po} are suitable positive feedback gains. Substituting (40) into (35) gives the closed-loop dynamic behaviour of the orientation error

$$\Delta\dot{\boldsymbol{\omega}}_{de} + k_{Vo}\Delta\boldsymbol{\omega}_{de} + k_{Po}\boldsymbol{\varepsilon}_{de} = \boldsymbol{0} \, . \tag{41}$$

Differently from (37), (39), the error system is nonlinear, and thus a Lyapunov argument is invoked below to ascertain its stability [18]. Let

$$V_2 = k_{Po}V_1 + \frac{1}{2}\Delta\boldsymbol{\omega}_{de}^T\Delta\boldsymbol{\omega}_{de} \tag{42}$$

be a positive definite Lyapunov function candidate, with V_1 as in (30). The time derivative of (42) along the trajectories of system (41) is

$$\dot{V}_2 = -k_{Vo}\Delta\boldsymbol{\omega}_{de}^T\Delta\boldsymbol{\omega}_{de} \tag{43}$$

where (16), (17) have been exploited.

Since $\dot{V}_2$ is only negative semi-definite, in view of LaSalle's theorem, the system asymptotically converges to the invariant set described by the two equilibria:

$$Q_1 = \{\eta_{de} = -1, \;\; \boldsymbol{\varepsilon}_{de} = \boldsymbol{0}, \;\; \Delta\boldsymbol{\omega}_{de} = \boldsymbol{0}\} \tag{44}$$

$$Q_2 = \{\eta_{de} = 1, \;\; \boldsymbol{\varepsilon}_{de} = \boldsymbol{0}, \;\; \Delta\boldsymbol{\omega}_{de} = \boldsymbol{0}\}. \tag{45}$$

Both Q_1 and Q_2 give the same mutual orientation $\boldsymbol{R}_d^e = \boldsymbol{I}$, i.e. the end-effector frame is aligned with the desired frame, so as wished. However, the equilibrium Q_1 is unstable. To see this, consider (42) which, in view of (43),

is a decreasing function. At the equilibrium in (44), it is

$$V_{2,\infty} = 4k_{Po}. \tag{46}$$

Take a small perturbation $\eta_{de} = -1 + \sigma$ around the equilibrium with $\sigma > 0$; then, it is $\varepsilon_{de}^T \varepsilon_{de} = 2\sigma - \sigma^2$. The perturbed Lyapunov function is

$$V_{2,\sigma} = 4k_{Po} - 2\sigma k_{Po} < V_{2,\infty} \tag{47}$$

and thus, since (42) is decreasing, V_2 will never return to $V_{2,\infty}$, implying that Q_1 is unstable. Therefore, the system must asymptotically converge to Q_2, which in turn implies that tracking of $\boldsymbol{R}_d$ and $\boldsymbol{\omega}_d$ is achieved.

The block scheme of the resulting dynamic control scheme using the Euler parameters is shown in Fig. 2.

V. IMPEDANCE CONTROL

When the robot's end effector is in contact with the environment, a suitable compliant behaviour has to be ensured. One of the most reliable strategies to manage the interaction is *impedance control* [5]. The goal is to keep the contact force limited both during transient and at steady state by acting on the end-effector displacement. Therefore, instead of tracking the desired frame specified by $\boldsymbol{p}_d$ and $\boldsymbol{R}_d$, it is worth considering a compliant frame specified by $\boldsymbol{p}_c$ and $\boldsymbol{R}_c$, and a mechanical impedance aimed at imposing a dynamic behavior for the position and orientation displacements between the above two frames.

With reference to the dynamic model (32) ($\boldsymbol{h} \neq \boldsymbol{0}$), the driving torques can be chosen as

$$\boldsymbol{\tau} = \boldsymbol{\tau}_m + \boldsymbol{J}^T(\boldsymbol{q})\boldsymbol{h} \tag{48}$$

with $\boldsymbol{\tau}_m$ as in (33), where contact force and moment measurements are used to compensate for the term $\boldsymbol{h}$ in (32). Substituting the control law (48) in (32) and accounting for the time derivative of (20) gives the same equations as (34), (35), where now $\boldsymbol{a}_p$ and $\boldsymbol{a}_o$ shall be designed to guarantee tracking of the compliant frame. In view of (36), for the position it is

$$\boldsymbol{a}_p = \ddot{\boldsymbol{p}}_c + k_{V_p}\Delta\dot{\boldsymbol{p}}_{ce} + k_{P_p}\Delta\boldsymbol{p}_{ce} \tag{49}$$

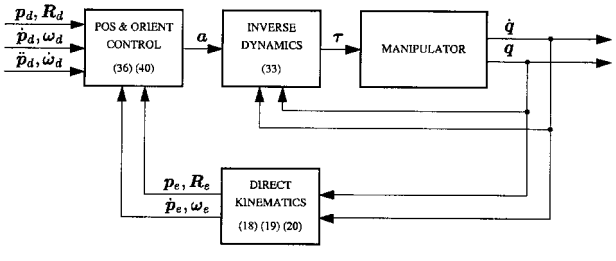

Fig. 2. Block scheme of dynamic control.

where $\Delta\boldsymbol{p}_{ce} = \boldsymbol{p}_c - \boldsymbol{p}_e$. For the orientation, it is worth discriminating between the Euler angles representation, via (38), i.e.

$$\boldsymbol{a}_o = \boldsymbol{T}(\boldsymbol{\varphi}_e)(\ddot{\boldsymbol{\varphi}}_c + k_{V_o}\Delta\dot{\boldsymbol{\varphi}}_{ce} + k_{P_o}\Delta\boldsymbol{\varphi}_{ce}) + \dot{\boldsymbol{T}}(\boldsymbol{\varphi}_e)\dot{\boldsymbol{\varphi}}_e\,, \tag{50}$$

where $\Delta\boldsymbol{\varphi}_{ce} = \boldsymbol{\varphi}_c - \boldsymbol{\varphi}_e$, and the Euler parameters representation, via (40), i.e.

$$\boldsymbol{a}_o = \dot{\boldsymbol{\omega}}_c + k_{Vo}\Delta\boldsymbol{\omega}_{ce} + k_{Po}\boldsymbol{\varepsilon}_{ce} \tag{51}$$

where $\boldsymbol{\varepsilon}_{ce}$ denotes the vector part of the Euler parameters associated with the mutual orientation between the compliant and the end-effector frame referred to the base frame, and $\Delta\boldsymbol{\omega}_{ce} = \boldsymbol{\omega}_c - \boldsymbol{\omega}_e$. Needless to say, the occurrence of representation singularities constitutes a problem for (50).

In order to ensure a suitable compliant behaviour during the interaction, a mechanical impedance between the contact force and moments and the end-effector position and orientation displacements of the compliant frame relative to the desired frame shall be designed. For the position part, the impedance equation can be chosen so as to enforce an equivalent mass-damper-spring behavior for the end-effector position displacement under the contact force $\boldsymbol{f}$ acting on the end effector, i.e.

$$\boldsymbol{M}_p\Delta\ddot{\boldsymbol{p}}_{cd} + \boldsymbol{D}_p\Delta\dot{\boldsymbol{p}}_{cd} + \boldsymbol{K}_p\Delta\boldsymbol{p}_{cd} = \boldsymbol{f}\,, \tag{52}$$

where $\Delta\boldsymbol{p}_{cd} = \boldsymbol{p}_c - \boldsymbol{p}_d$, and $\boldsymbol{M}_p$, $\boldsymbol{D}_p$, $\boldsymbol{K}_p$ are positive definite matrices. In particular, the stiffness matrix $\boldsymbol{K}_p$ can be decomposed as

$$\boldsymbol{K}_p = \boldsymbol{U}_p\boldsymbol{\Gamma}_p\boldsymbol{U}_p^T\,, \tag{53}$$

where $\boldsymbol{\Gamma}_p = \mathrm{diag}\{\gamma_{p1}, \gamma_{p2}, \gamma_{p3}\}$ is the eigenvalue matrix and $\boldsymbol{U}_p = [\boldsymbol{u}_{p1}\ \boldsymbol{u}_{p2}\ \boldsymbol{u}_{p3}]$ is the (orthogonal) eigenvector matrix. Then, considering a position displacement of length λ along the i-th eigenvector leads to

$$\boldsymbol{f}_E = \boldsymbol{K}_p\Delta\boldsymbol{p}_{cd} = \gamma_{pi}\lambda\boldsymbol{u}_{pi} \tag{54}$$

which represents an elastic force along the same $\boldsymbol{u}_{pi}$ axis. This implies that the translational stiffness matrix can be expressed in terms of three parameters γ_{pi} representing the stiffness along three principal axes $\boldsymbol{u}_{pi}$, and in turn it allows the translational stiffness to be specified in a consistent way with the task geometry [19].

With reference to the Euler angles representation, the rotational part of the impedance at the end effector can be formally defined in the same way as for the positional part (52), i.e.

$$\boldsymbol{M}_o\Delta\ddot{\boldsymbol{\varphi}}_{cd} + \boldsymbol{D}_o\Delta\dot{\boldsymbol{\varphi}}_{cd} + \boldsymbol{K}_o\Delta\boldsymbol{\varphi}_{cd} = \boldsymbol{T}^T(\boldsymbol{\varphi}_c)\boldsymbol{\mu}\,, \tag{55}$$

where $\Delta\boldsymbol{\varphi}_{cd} = \boldsymbol{\varphi}_c - \boldsymbol{\varphi}_d$, and $\boldsymbol{M}_o$, $\boldsymbol{D}_o$, $\boldsymbol{K}_o$ are positive definite matrices describing the generalized inertia, rotational

damping, rotational stiffness, respectively, and μ is the contact moment at the end effector; all the above quantities have been referred to the base frame, and $\boldsymbol{T}^T(\boldsymbol{\varphi}_c)$ is the transformation matrix needed to express the moment in terms of an equivalent operational space quantity, via a kineto-static duality concept based on (3).

Notice that, differently from (52), the dynamic behaviour for the rotational part is not absolutely determined by the choice of the impedance parameters but it does also depend on the orientation of the compliant frame with respect to the base frame through the matrix $\boldsymbol{T}^T(\boldsymbol{\varphi}_c)$. Moreover, Eq. (55) becomes ill-defined in the neighbourhood of a representation singularity; in particular, at such a singularity, moment components in the null space of $\boldsymbol{T}^T$ do not generate any contribution to the dynamics of the orientation displacement, leading to a possible build-up of large values of contact moment.

The effect of the rotational stiffness can be better understood by considering an infinitesimal orientation displacement between the compliant and the desired frame. From (55), in the absence of representation singularities, the elastic moment is

$$\boldsymbol{\mu}_E = \boldsymbol{T}^{-T}(\boldsymbol{\varphi}_c)\boldsymbol{K}_o\Delta\boldsymbol{\varphi}_{cd} \,. \tag{56}$$

In the case of an infinitesimal orientation displacement about $\boldsymbol{\varphi}_d$, it is

$$\begin{aligned} \mathrm{d}(\Delta\boldsymbol{\varphi}_{cd}) &= (\dot{\boldsymbol{\varphi}}_c - \dot{\boldsymbol{\varphi}}_d)\big|_{\boldsymbol{\varphi}_c = \boldsymbol{\varphi}_d}\mathrm{d}t \\ &= \boldsymbol{T}^{-1}(\boldsymbol{\varphi}_d)\Delta\boldsymbol{\omega}_{cd}\mathrm{d}t \,, \end{aligned} \tag{57}$$

where $\Delta\boldsymbol{\omega}_{cd} = \boldsymbol{\omega}_c - \boldsymbol{\omega}_d$ is the relative angular velocity between the two frames. Folding (57) into (56) written for an infinitesimal displacement $\mathrm{d}(\Delta\boldsymbol{\varphi}_{cd})$ gives

$$\begin{aligned} \boldsymbol{\mu}_E &= \boldsymbol{T}^{-T}(\boldsymbol{\varphi}_c)\boldsymbol{K}_o\boldsymbol{T}^{-1}(\boldsymbol{\varphi}_d)\Delta\boldsymbol{\omega}_{cd}\mathrm{d}t \\ &\simeq \boldsymbol{T}^{-T}(\boldsymbol{\varphi}_d)\boldsymbol{K}_o\boldsymbol{T}^{-1}(\boldsymbol{\varphi}_d)\Delta\boldsymbol{\omega}_{cd}\mathrm{d}t \end{aligned} \tag{58}$$

where the first-order approximation $\boldsymbol{T}^{-T}(\boldsymbol{\varphi}_c) \simeq \boldsymbol{T}^{-T}(\boldsymbol{\varphi}_d)$ has been made. Eq. (58) reveals that the equivalent rotational stiffness between the orientation displacement and the elastic moment depends on the desired end-effector orientation. It follows that a property of geometric consistency similar to that of the elastic force (54) is lost when considering the elastic moment (56), that is, the eigenvectors of the matrix $\boldsymbol{K}_o$ do not represent the three principal axes for the rotational stiffness [19].

The drawbacks of representation singularities and task geometry consistency can be mitigated by adopting an alternative orientation displacement which is based on the Euler angles extracted from the rotation matrix describing the mutual orientation between the compliant and the desired frame; as above, the advantage is that representation singularities occur only for large orientation errors, but task geometric consistency is ensured only for a diagonal stiffness matrix [10].

In order to overcome the problem of representation singularities and task geometric consistency, the rotational impedance can be formulated in terms of the relative angular velocity and the Euler parameters between the compliant and the desired frame, i.e. in the form

$$\boldsymbol{M}_o\Delta\dot{\boldsymbol{\omega}}^d_{cd} + D_o\Delta\boldsymbol{\omega}^d_{cd} + \boldsymbol{K}'_o\boldsymbol{\varepsilon}^d_{cd} = \boldsymbol{\mu}^d \,, \tag{59}$$

where the equivalent rotational stiffness matrix is

$$\boldsymbol{K}'_o = 2\boldsymbol{E}^T(\eta_{cd}, \boldsymbol{\varepsilon}^d_{cd})\boldsymbol{K}_o \tag{60}$$

with $\boldsymbol{E}$ as in (10). The expression of $\boldsymbol{K}'_o$ is motivated by energy arguments to be found in [10]. Notice that the rotational part of the impedance equation has been derived in terms of quantities all referred to the desired frame; this allows the impedance behavior to be effectively expressed in terms of the relative orientation of the compliant frame with respect to the desired frame, no matter what the absolute orientation of the desired frame with respect to the base frame is.

As above, the effect of the rotational stiffness can be better understood by considering an infinitesimal orientation displacement between the compliant and the desired frame, i.e.

$$\begin{aligned} \mathrm{d}\boldsymbol{\varepsilon}^d_{cd} &= \dot{\boldsymbol{\varepsilon}}^d_{cd}\big|_{\{\eta_{cd}=1,\, \boldsymbol{\varepsilon}^d_{cd}=0\}}\mathrm{d}t \\ &= \frac{1}{2}\Delta\boldsymbol{\omega}^d_{cd}\,\mathrm{d}t \end{aligned} \tag{61}$$

where the propagation rule (17) has been exploited. From (59), the elastic moment is

$$\begin{aligned} \boldsymbol{\mu}^d_E &= \boldsymbol{E}^T(\mathrm{d}\eta_{cd}, \mathrm{d}\boldsymbol{\varepsilon}^d_{cd})\boldsymbol{K}_o\mathrm{d}\Delta\boldsymbol{\omega}^d_{cd}\,\mathrm{d}t \\ &\simeq \boldsymbol{K}_o\Delta\boldsymbol{\omega}^d_{cd}\,\mathrm{d}t \,, \end{aligned} \tag{62}$$

where the first-order approximation $\boldsymbol{E}^T(\mathrm{d}\eta_{cd}, \mathrm{d}\boldsymbol{\varepsilon}^d_{cd}) \simeq \boldsymbol{I}$ has been made. Eq. (62) clearly shows how the equivalent rotational stiffness is independent of the desired end-effector orientation, and the problem of representation singularity is avoided.

As regards the property of geometric consistency, the stiffness matrix $\boldsymbol{K}_o$ can be decomposed as

$$\boldsymbol{K}_o = \boldsymbol{U}_o\boldsymbol{\Gamma}_o\boldsymbol{U}_o^T \tag{63}$$

where $\boldsymbol{\Gamma}_o = \mathrm{diag}\{\gamma_{o1}, \gamma_{o2}, \gamma_{o3}\}$ is the eigenvalue matrix and $\boldsymbol{U}_o = [\boldsymbol{u}_{o1}\ \boldsymbol{u}_{o2}\ \boldsymbol{u}_{o3}]$ is the (orthogonal) eigenvector matrix. Then, considering an orientation displacement by an angle ϑ about the i-th eigenvector gives the Euler parameters

$$\left\{ \eta_{cd} = \cos\frac{\vartheta}{2},\ \boldsymbol{\varepsilon}^d_{cd} = \sin\frac{\vartheta}{2}\boldsymbol{u}_{oi} \right\} , \tag{64}$$

leading to

$$\boldsymbol{\mu}_E^d = \gamma_{oi} \sin \vartheta \, \boldsymbol{u}_{oi} \tag{65}$$

which represents an elastic moment about the same $\boldsymbol{u}_{oi}$ axis. This implies that the rotational stiffness matrix can be expressed in terms of three parameters γ_{oi} representing the stiffness about three principal axes $\boldsymbol{u}_{oi}$, i.e. in a consistent way with the task geometry.

Eqs. (52), (59) describe a six-degree-of-freedom impedance behaviour where the translational part is decoupled from the rotational part. A more general impedance equation can be derived by introducing coupling elastic terms, as discussed in [20].

In the case of free motion, it is worth finding the equilibria of the rotational impedance equation (59). These should occur whenever the orientation of the compliant frame coincides with that of the desired frame. If $\boldsymbol{\mu}^d = \boldsymbol{0}$, then the equilibria of (59}) are described by

$$\boldsymbol{\mu}_E^d = 2(\eta_{cd}\boldsymbol{K}_o\boldsymbol{\varepsilon}_{cd}^d + \boldsymbol{S}(\boldsymbol{\varepsilon}_{cd}^d)\boldsymbol{K}_o\boldsymbol{\varepsilon}_{cd}^d) = \boldsymbol{0} \tag{66}$$

where (60) has been exploited.

By observing that the two terms in (66) are mutually orthogonal, the equilibria are Q_1 in (44), Q_2 in (45), and

$$Q_3 = \{\eta_{cd} = 0, \ \boldsymbol{\varepsilon}_{cd}^d : \boldsymbol{K}_o\boldsymbol{\varepsilon}_{cd}^d = \gamma_o\boldsymbol{\varepsilon}_{cd}^d, \ \left\| \boldsymbol{\varepsilon}_{cd}^d \right\| = 1, \ \Delta\boldsymbol{\omega}_{cd}^d = \boldsymbol{0}\} \tag{67}$$

where $\gamma_o > 0$ denotes an eigenvalue of matrix $\boldsymbol{K}_o$.

The stability of the system can be analyzed by considering the positive definite Lyapunov function candidate

$$V_3 = \frac{1}{2}\Delta\boldsymbol{\omega}_{cd}^{dT}\boldsymbol{M}_o\Delta\boldsymbol{\omega}_{cd}^d + 2\boldsymbol{\varepsilon}_{cd}^{dT}\boldsymbol{K}_o\boldsymbol{\varepsilon}_{cd}^d \, . \tag{68}$$

Computing the time derivative of V_3 along the trajectories of the system (59), (60) yields

$$\dot{V}_3 = -\Delta\boldsymbol{\omega}_{cd}^{dT}\boldsymbol{D}_o\Delta\boldsymbol{\omega}_{cd}^d \tag{69}$$

which is negative semidefinite. In view of LaSalle's theorem, the system asymptotically converges to the invariant set $Q_1 \cup Q_2 \cup Q_3$.

The equilibria in Q_3 are unstable. To see this, consider the function (68) which, in view of (69), is a decreasing function. At any of the equilibria in (67), it is

$$V_{3,\infty} = 2\gamma_o\boldsymbol{\varepsilon}_{cd}^{dT}\boldsymbol{\varepsilon}_{cd}^d = 2\gamma_{oi} \tag{70}$$

where (6) has been used. Consider a small perturbation around the equilibrium with $\eta_{cd} = \sigma$, $\boldsymbol{\varepsilon}_{cd}^d$ such that $\boldsymbol{\varepsilon}_{cd}^{dT}\boldsymbol{\varepsilon}_{cd}^d = 1 - \sigma^2$, $\Delta\boldsymbol{\omega}_{cd}^d = \boldsymbol{0}$ and $\boldsymbol{K}_o\boldsymbol{\varepsilon}_{cd}^d = \gamma_o\boldsymbol{\varepsilon}_{cd}^d$. The perturbed Lyapunov function is

$$V_{3,\sigma} = 2\gamma_o(1 - \sigma^2) < V_{3,\infty} \tag{71}$$

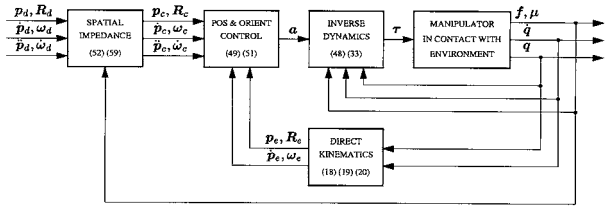

Fig. 3. Block scheme of impedance control.

and thus, since (68) is decreasing, V_3 will never return to $V_{3,\infty}$, implying that those equilibria are all unstable. Notice that, at such equilibria, the compliant frame is anti-aligned with the desired frame with respect to the equivalent axis of the mutual rotation $\boldsymbol{R}_c^d$ between the two frames.

It can be concluded that $\boldsymbol{\varepsilon}_{cd}^d$ must converge to $Q_1 \cup Q_2$. Notice, however, that the equilibrium Q_1 corresponds to a rotation of 2π about the equivalent axis, but such a large orientation displacement between the compliant and the desired frame is of no interest for practical implementation of impedance control.

The block scheme of the resulting impedance control scheme using the Euler parameters is shown in Fig. 3. It is worth observing the presence of an inner motion loop, whose references $\boldsymbol{p}_c$, $\boldsymbol{R}_c$ and its associated velocities can be computed by forward integration of the translational and the rotational impedance equations (52), (59) with input $\boldsymbol{h}$ available from the force/torque sensor. Remarkably, the gains of the motion loop in (49), (51) can be set independently of the impedance parameters so as to provide accurate position tracking of $\boldsymbol{p}_c$, $\boldsymbol{R}_c$ and good disturbance rejection [21].

VI. CONCLUSION

The role of Euler parameters in robot control has been discussed in this paper. The advantages over the Euler angles typically used in the operational space framework have been demonstrated in avoiding representation singularities for the problems of kinematic control and dynamic control. In addition to that, task geometry consistency has been demonstrated for the impedance control problem when using Euler parameters. The theoretical analysis of the various control schemes has been provided in a unifying perspective, whereas a thorough numerical analysis and experimental validation on an industrial robot of kinematic control, dynamic control and impedance control based on Euler parameters can be found in [8], [9], [10], respectively.

REFERENCES

1. Khatib, O., "A Unified Approach for Motion and Force Control of Robot Manipulators: The Operational Space Formulation," *IEEE J. Rob. Autom.*, Vol. 3, pp. 43-53 (1987).

2. Sciavicco, L. and B. Siciliano, *Modeling and Control of Robot Manipulators*, McGraw-Hill, New York, NY (1996).
3. Siciliano, B., "A Closed-loop Inverse Kinematic Scheme for On-line Joint-based Robot Control," *Robotica*, Vol. 8, pp. 231-243 (1990).
4. Luh, J.Y.S., M.W. Walker and R.P.C. Paul, "Resolved-acceleration Control of Mechanical Manipulators," *IEEE Trans. Automat. Contr.*, Vol. 25, pp. 468-474 (1980).
5. Hogan, H., "Impedance Control: An Approach to Manipulation, Parts I-III," *ASME J. Dyn. Syst., Meas. Contr.*, Vol. 107, pp. 1-24 (1985).
6. Murray, R.M., Z. Li and S.S. Sastry, *A Mathematical Introduction to Robotic Manipulation*, CRC Press, Boca Raton, FL (1994).
7. Yuan, J.S.-C. "Closed-loop Manipulator Control Using Quaternion Feedback," *IEEE J. Robo. Autom.*, Vol. 4, pp. 434-440 (1988).
8. Chiaverini, S. and B. Siciliano, "The Unit Quaternion: A Useful Tool for Inverse Kinematics of Robot Manipulators," *Syst. Anal. Modell. Simul.*, in press (1999).
9. Caccavale, F., C. Natale, B. Siciliano and L. Villani, "Resolved-acceleration Control of Robot Manipulators: A Critical Review with Experiments," *Robotica*, Vol. 16, pp. 565-573 (1998).
10. Caccavale, F., C. Natale, B. Siciliano and L. Villani, "Six-DOF Impedance Control Based on Angle/axis Representations," *IEEE Trans. Rob. Autom.*, Vol. 15, pp. 289-300 (1999).
11. Roberson, R.E. and R. Schwertassek, *Dynamics of Multibody Systems*, Springer-Verlag, Berlin (1988).
12. Shepperd, S.W., "Quaternion from Rotation Matrix," *AIAA J. Guid. Contr.*, Vol. 1, pp. 223-224 (1978).
13. Nakamura, Y., *Advanced Robotics: Redundancy and Optimization*, Addison-Wesley, Reading, MA (1991).
14. Chiaverini, S., B. Siciliano and O. Egeland, "Review of the Damped Least-squares Inverse Kinematics with Experiments on an Industrial Robot Manipulator," *IEEE Trans. Contr. Syst. Technol.*, Vol. 2, pp. 123-134 (1994).
15. Caccavale, F. and P. Chiacchio, "Identification of Dynamic Parameters and Feedforward Control for a Conventional Industrial Manipulator," *Control Eng. Pract.*, Vol. 2, pp. 1039-1050 (1994).
16. Wampler, C.W. and L.J. Leifer, "Applications of Damped Least-squares Methods to Resolved-rate and Resolved-acceleration Control of Manipulators, *ASME J. Dyn. Syst., Meas. Contr.*, Vol. 110, pp. 31-38 (1988).
17. Hsu, P., J. Hauser and S. Sastry, "Dynamic Control of Redundant Manipulators," *J. Rob. Syst.*, Vol. 6, pp. 133-148 (1989).
18. Wen, J.T.-Y. and K. Kreutz-Delgado, "The Attitude Control Problem," *IEEE Trans. Automat. Contr.*, Vol. 36, pp. 1148-1162 (1991).
19. Fasse, E.D. and J.F. Broenink, "A Spatial Impedance Controller for Robotic Manipulation," *IEEE Trans. Rob. Autom.*, Vol. 13, pp. 546-556 (1997).
20. Caccavale, F., B. Siciliano and L. Villani, "Robot Impedance Control with Nondiagonal Stiffness," *IEEE Trans. Automat. Contr.*, Vol. 45 (2000).
21. Lu, W.-S. and Q.-H. Meng, "Impedance Control with Adaptation for Robotic Manipulators," *IEEE Trans. Rob. Autom.*, Vol. 7, pp. 408-415 (1991).

Fabrizio Caccavale was born in Naples, Italy, on November 14, 1965. He received the *Laurea* degree and the *Research Doctorate* degree in Electronic Engineering from the University of Naples in 1993 and 1997, respectively. Since 1997 he has been working at the Faculty of Engineering of the University of Naples, where he is currently *Post-Doctorate Fellow* of Robotics in the Department of Computer and Systems Engineering. From April to October 1996 he was a visiting scholar at the Department of Electrical and Computer Engineering of Rice University. His research interests include manipulator inverse kinematics techniques, cooperative robot manipulation, and nonlinear control of mechanical systems. He has published more than 30 journal and conference papers.

Bruno Siciliano was born in Naples, Italy, on October 27, 1959. He received the *Laurea* degree and the *Research Doctorate* degree in Electronic Engineering from the University of Naples in 1982 and 1987, respectively. Since 1983 he has been working at the Faculty of Engineering of the University of Naples, where he is currently *Associate Professor* of Robotics in the Department of Computer and Systems Engineering. Since 1993 he is an *Adjunct Professor* of Systems Theory in the Department of Information and Electrical Engineering of the University of Salerno. From September 1985 to June 1986 he was a visiting scholar at the School of Mechanical Engineering of the Georgia Institute of Technology. His research interests include manipulator inverse kinematics techniques, redundant manipulator control, modeling and control of flexible arms, force/motion control of manipulators, and cooperative robot manipulation. He has published more than 150 journal and conference papers, he is co-author of the books *Modeling and Control of Robot Manipulators with Solutions Manual* (McGraw-Hill, 1996), and *Theory of Robot*

Control (Springer-Verlag, 1996), and he is co-editor of the book *Control Problems in Robotics and Automation* (Springer-Verlag, 1998). He has delivered more than 60 invited seminars and presentation at international institutions. Professor Siciliano has served as an *Associate Editor* of the *IEEE Transactions on Robotics and Automation* from 1991 to 1994, and as an *Associate Technical Editor* of the *ASME Journal of Dynamic Systems, Measurement, and Control* from 1994 to 1998. He is also on the Editorial Advisory Boards of *Robotica* and the *JSME International Journal*. He is an Associate Member of ASME and a Senior Member of IEEE. Since 1996 he is an *Administrative Committee Member* of the *IEEE Robotics and Automation Society* (re-elected in 1999), and *Chair* of the *Technical Committee on Manufacturing and Automation Robotic Control* of the IEEE *Control Systems Society*. In February 1999 he has been appointed *Vice-President for Publications* of the *IEEE Robotics and Automation Society*. He has been on the program committees of several international robotics conferences, he has been *Program Chair* of the *IEEE International Workshop on Control Problems in Robotics and Automation: Future Directions* (1997), *Program Vice-Chair* of the *IEEE International Conference on Robotics and Automation* (1998, 1999), and *General Co-Chair of the IEEE/ASME International Conference on Advanced Intellingent Mechatronics* (1999).

Luigi Villani was born in Avellino, Italy, on December 5, 1966. He received the *Laurea* degree and the *Research Doctorate* degree in Electronic Engineering from the University of Naples in 1992 and 1996, respectively. Since 1996 he has been working at the Faculty of Engineering of the University of Naples, where he is currently *Post-Doctorate Fellow* of Robotics in the Department of Computer and Systems Engineering. From June to October 1995 he was a visiting scholar at the Laboratoire d'Automatique de Grenoble, Institut National Polytechnique de Grenoble. His research interests include force/motion control of manipulators, adaptive and nonlinear control of mechanical systems. He has published more than 35 journal and conference papers, and he is co-author of the booklet *Solutions Manual to Modeling and Control of Robot Manipulators*, McGraw-Hill, New York, 1996. He is a Member of IEEE.